Advanced Technologies for Hypersonic, Propulsive, Energetic and Reusable Platforms
REU-HYPER 2019
28 May – 2 August 2019, Orlando, United States

Materials Characterization and Evaluation of Oxide-Oxide Ceramic Matrix Composites

Daniel Poljak[1]
Derek Saltzman[2]

[1]University of Florida, Materials Science and Engineering
[2]University of Central Florida, Mechanical and Aerospace Engineering

ABSTRACT

Ceramic matrix composites (CMC's) have been heavily studied over the last few decades due to their opportunity to enable aerospace applications. Their inherent low density and superior thermal properties make them an ideal candidate for hypersonic and propulsive technologies. This study produced replicable oxide-oxide CMC parts that were tested to evaluate material, and mechanical properties of in-house manufactured composite parts. The studied material was Axiom 7810-610, a Nextel 610 fiber impregnated with an aluminosilicate matrix bound in a plain weave pattern. The material had an autoclave treatment to cure the layup. This was followed by pyrolysis in a kiln to change the microstructure when exposed to high temperatures. The final parts resulted in a CMC, whose microstructure was analyzed via SEM/EDS as well as XRD. Samples went through bend tests to compare to industry references. Future work to be done with more thermo-mechanical testing as well as corrosion testing for unique oxidizing environments.

NOMENCLATURE

$$\sigma = maximum\ bending\ strength$$
$$M = maximum\ bending\ moment$$
$$I = moment\ of\ inertia$$
$$c = normal\ distance\ from\ neutral\ axis\ to\ furthest\ point\ of\ segment$$

1. INTRODUCTION

Composites materials can be defined as the combination of two physically and/or chemically distinct materials, whose characteristics cannot be defined solely by any separated component [1]. Thus, when combined result in augmented properties completely unique to that specific combination. Generally, a composite is composed of a matrix phase which acts as a medium to transfer applied loads to the surrounded reinforcement (fibril) material. One can have reinforcement material in the form of particles, flakes, whiskers, short fibers, continuous fibers, or sheets. Generally (and in this study) most reinforcements used in composites utilize a fibrous form. This is because materials are stronger and stiffer in the fibrous form than in any other form [1]. The strength of the composite made is most often dictated by the fiber direction, as they bear most of the load. These long fibers are bundled in groups known as "tows" which can be woven into patterns and sold in rolls. When combined with a resin these laminate composites are extremely light and strong, making them favorable for many applications.

Despite the quick appeal, every material has its benefits and limitations. The damage mechanisms in composites are very complex and can involve one or more failure modes at a time. Delamination, fiber breakage, matrix cracking, and fiber-matrix debonding are all damages that give more information about the composite itself or the load it was under. These damages significantly reduce the load bearing capability of composite structures, which generally leads to premature failure [2]. These damages can form quickly in the presence of excessive porosity. Pores can be formed by inadequate manufacturing technique discussed later, or product impurities. They act as stress concentrators and have a significant impact on the quality of composite (material performance). Delamination is one of the most commonly studied failure modes. It can occur due to product flaws, manufacturing errors, or even damages caused in the handling of the final composite product. The specificity and sensitivity of composite fabrication has

made it difficult for adoption into the aerospace industry [2]. It also makes it specifically difficult for prototyping in research labs for continued development.

Aerospace applications require materials with high specific strength and thermal resistance. Out of the many possible types of composites available ceramic matrix composites (CMC's) have been rapidly taking over this material need in the last decade [2]. CMC's can be divided into two primary categories: non-oxide CMC's and oxide-oxide CMC's. This study focuses on oxide-oxide CMC's as non-oxide are susceptible to oxidation in high temperature and corrosive environments. Oxidation in turn damages the integrity of fiber/matrix bonding, significantly reducing its lifetime [3]. Additionally, Si-C non-oxide CMC's utilized in industrial applications are extremely expensive.

There are many components within aerospace technologies that do not require the same higher temperature capabilities. Components such as exhaust filters, exchange components, thrust chambers, and exit nozzles are already being developed using oxide-oxide CMC's [4, 5]. These parts operate in an extremely high temperature, and are exposed to an oxidizing environment, making them perfect for oxide-oxide CMC's. These CMC's are much lighter than their metal counterparts and exhibit less mechanical deformation at higher temperatures. In space applications, an increase of 200°C fuel turbo-pump temperature is projected to a 2.5% increase in thrust [6]. The efficiency and thrust of propulsive engines are limited by the allowable fuel turbopump temperature. Reducing weight to aerospace structures, while allowing higher operating temperatures at no significant loss of mechanical properties in a highly oxidizing environment, is a task most materials cannot simply do. Oxide-oxide CMC's have proven to be perform better than traditional engine components exposed to high temperature, oxidizing environments.

2. BACKGROUND

One of the challenges in aerospace applications is the need for low density, high temperature materials of hot section parts in order to maximize fuel efficiency and provide maximum thrust. However, few materials can withstand temperatures in excess of 850°C without creep and oxidation affecting the materials' structural integrity. This study aims at addressing the need for a material that can withstand high temperatures and operate in an oxidizing environment, specifically as a heat exchanger component in extreme environments.

Traditionally, nickel based super alloys (Inconel 617) have been utilized for high temperature, load bearing components of aerospace structures. Studies show that the temperature boundary of utilizing Inconel is 850°C. Above such temperature creep and oxidation become a significant factor causing rupture in approximately 10,000 hours bearing a 35 MPa stress [7]. Recently more focus has been placed in low density, more advanced materials, which have a significantly higher creep tolerance. Non oxide CMC's, and oxide-oxide CMC's have been the focus of new high temperature aerospace applications. Both materials consist of fibers bundled in "tows" which are wrapped in a woven pattern. The said fabric pattern is impregnated with proprietary slurries which upon curing and pyrolysis form the ceramic matrix. The fibers allow for enhanced fracture toughness to typical monolithic ceramics. This technology is limited by the grain size and phase transition temperatures of the ceramic fibers.

Non oxide CMC's such as Si-C offer superior thermal and mechanical properties under a non-oxidizing environment. Non-oxide CMC's used for aerospace must exhibit creep strains lower than 1 percent after 10,000 hours of service at 100 MPa [8]. These numbers are not possible under an oxidizing environment. Therefore, the integrity is dependent on the quality of environmental barrier coating. Meanwhile, oxide-oxide CMC's can withstand a variety of environmental conditions from volatile gases, to corrosive liquids like molten salt. The need for multipurpose, long lasting parts, motived this study to examine the benefits of oxide-oxide CMC's to chemically corrosive and extremely high temperature heat exchanger parts for aerospace and energy applications.

The primary material being investigated is Axiom 7810-610 specifically DF-11 (5HS 3000). The composite is impregnated with Axiom 7810 proprietary aluminosilicate slurry (forms matrix), along with Nextel ™ 610 fiber. DF-11 5HS indicates a plain weave pattern, coupled with a thickness of 3000 denier. Denier (D) is a measurement that indicates the thickness of each strand of fiber (grams per 9000 m of fiber).

Axiom offers the thinnest of 1500 D which also costs the most to process and manufacture. The same material in 3000 D can be made 20% cheaper and still be used for structural applications and contouring surfaces [9]. Nextel ™ 610 exhibit creep strains of less than 1 percent after 10,000 hours under a stress of 69 MPa. The Nextel ™ 610 fiber is primarily used for structural applications and is formed of >99% alpha aluminium oxide large polycrystalline grain sizes which allow for greater strength and less creep resistance than Nextel ™ 720 [10].

Traditionally, a key issue with CMC technology especially as it grows into industry is the variability in quality. Formation of pores lead to stress concentration regions that can vary its performance, making it less than favourable for most industry applications [11]. Within research this limitation is difficult to overcome given limited equipment availability and quality. Even when starting with the pre-impregnated material researchers must entertain stages industry conducts autonomously, by hand. This leads to great variation simply due to an inconsistency in researchers' methodology. This study is

focused on addressing that gap, as it focused on making replicable parts in house form a replicable process. This is ensured through characterization of microstructure, after which thermo-mechanical testing will be compared to Axiom's data sheet. Given the samples are within a reasonable error (15%), a heat exchanger part will be manufactured and tested with molten salt flowing through as the medium.

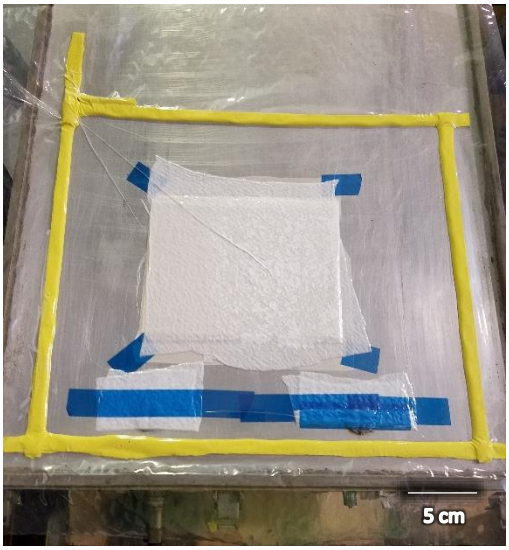

Fig. 1: Vacuum bag procedure for AX-7810-610

3. MATERIALS AND METHODS

The research was conducted in a two-step process. The first step required the in-house manufacturing from pre-preg composite to a final quality CMC part. The second step required material and mechanical characterization of the final CMC from Axiom 7810-610.

To ensure low porosity the manufacturing process had to be well documented and executed for replicable results. First the tray which held the sample needed to be waxed with mold release. Taped regions were laid down to note the area in which the sample would fit on the tray. Between layers of mold release specific dimensions of the Axiom 7810-610 roll were cut. From this sample size the specific testing specimens needed (ASTM standard) were later cut out to minimize wasted material. The lay-up required careful layer by layer stacking on the waxed tray to reduce air gaps and potential regions for delamination. Once laid up, the sample had a Teflon™ layer of fabric (release film) laid over it to allow excess resin to be pulled by the vacuum from the CMC part. Over the release film another cotton-like fabric (bleeder fabric) was placed to catch and absorb the bled through resin. More bleeder fabric was placed over the vacuum ports to protect the vacuum from any excess resin which made it past both layers. The blue tape was removed from the tray leaving a clean metal surface (rather than a slick waxed layer) to lay down yellow tacky tape. The tacky tape held down the vacuum bag which was carefully pressed against the tape. With the last part of vacuum bag to be laid down a pleat was made to reduce crimping on the edges which would be the cause of leaks.

This vacuum bag set up was then connected to a vacuum to ensure a strong vacuum could be drawn. If the reading was within 15 percent of the set vacuum, the bagged layup was considered ready for autoclave treatment. The set up was placed in the autoclave to cure under vacuum, pressure, and heated at 177°C. After curing the panel was cut into required sample dimensions for testing. Parts were weighed, measured, and recorded before being placed in the kiln for pyrolysis at a prolonged time under 1093°C.

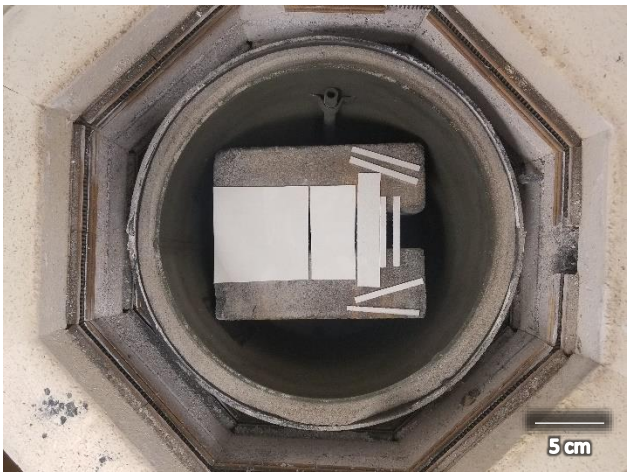

Fig. 2: Pre-cut sample pieces in the kiln for pyrolysis

This process was verified through the analysis of the cross section under SEM to analyze matrix/fiber bonding, as well as porosity. EDS was performed to detect elemental composition of both the fibers and matrix phase which was useful in screening for XRD. XRD was done assuming traces of Al, O, and Si. This analysis confirmed the details of the crystal structure formed. After materials characterization, three-point bending was conducted to compare to data from similar CMC's by Axiom.

4. RESULTS AND DISCUSSION

A. SEM

Scanning Electron Microscopy (SEM) was performed using a Zeiss ULTRA 55 Field Emission Gun SEM at the Materials Characterization Facility. This machine was also used to perform Energy Dispersive Spectroscopy (EDS) with a Noran System 7 EDS system with Silicon Drift Detector.

Once the sample was mounted a thin 10 nm layer of gold was sputter coated on to the surface to reduce charging effects on the non-conductive, ceramic surface. SEM was used to analyze the porosity of the matrix phase for the cross section of the composite. The machine utilized an

electron beam to obtain information about the material and its surface. EDS determined the elemental composition of the material by detecting the energy released from atoms as they are hit with an electron beam. EDS of this machine was limited to a lateral resolution of 5 microns which was significant as fibers were merely 10 to 12 micron in diameter.

The initial images taken from training provided clear images of the fiber shape surrounded by a damaged matrix (Fig. 3). This sample was not properly prepared and broken to reveal the cross section immediately before analysis due to improper sizing. This made it difficult to determine if the porosity observed was representative of the samples made in the lab. Additionally, the variation in the length of protruding fibers at the cross section resulted in limited resolution of specific areas. A lower surface roughness was needed to produce an image with better overall resolution.

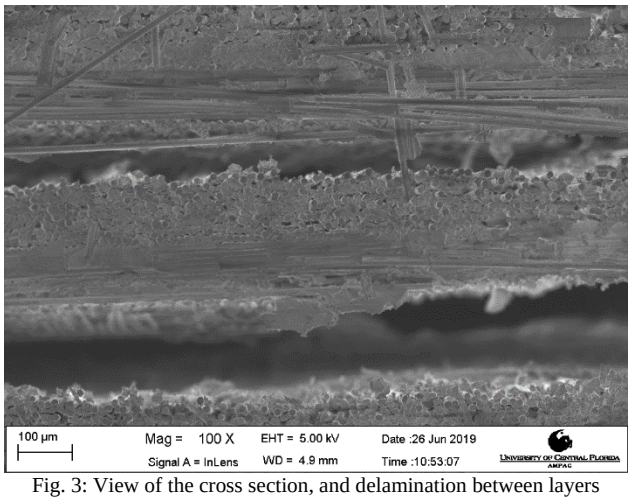

Fig. 3: View of the cross section, and delamination between layers

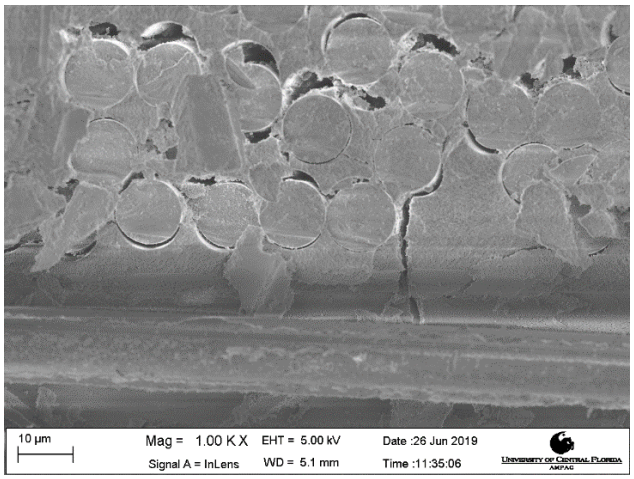

Fig. 4: Zoomed image focused on a small dense bundle of fibers, displaying matrix crack propagation between fibers of a single layer

In order to obtain a more focused and lower surface roughness the cross section of a new sample was polished after breaking. Polishing allowed for material removal of the initial damaged layers due to cracking and other handling. Polishing was done by hand at 15 seconds per grit. Grit size was increased from 220, 320, 400, and 600: all using a ceramic alumina material. Once surface was evenly removed P1000, and P1500 were used which utilized silicon carbide to smooth the finished surface. This resulted in a relatively even surface shown in Fig. 5, with lower surface roughness (better resolution). After polishing the cross section was blasted with a nitrogen to remove loose particles. Fig. 5-7b show the cross section of the polished sample.

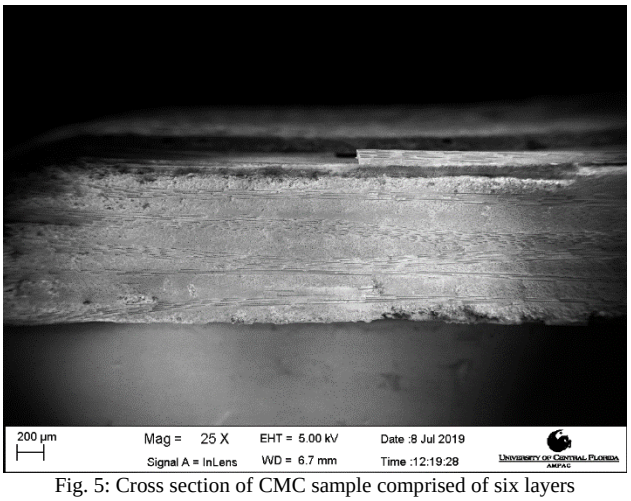

Fig. 5: Cross section of CMC sample comprised of six layers

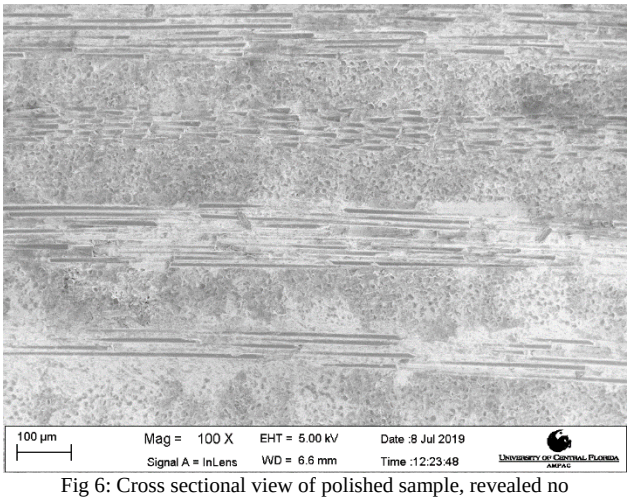

Fig 6: Cross sectional view of polished sample, revealed no delamination between adjacent layers

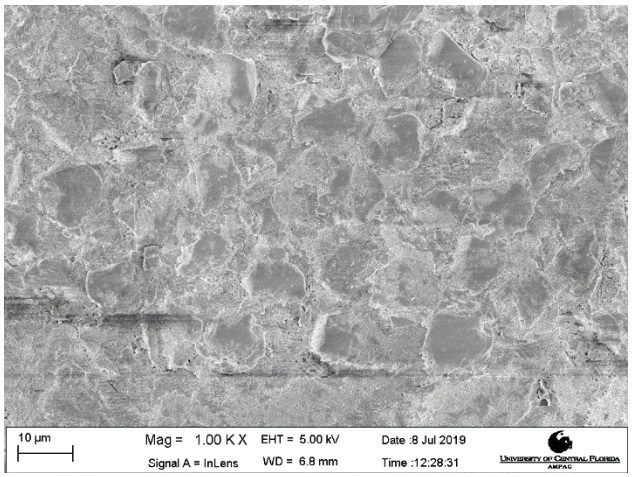

Fig. 7a: Zoomed InLens view of fibers pointed out of the plane of the page, revealed fibers with a damage morphology due to polishing with a filled matrix phase

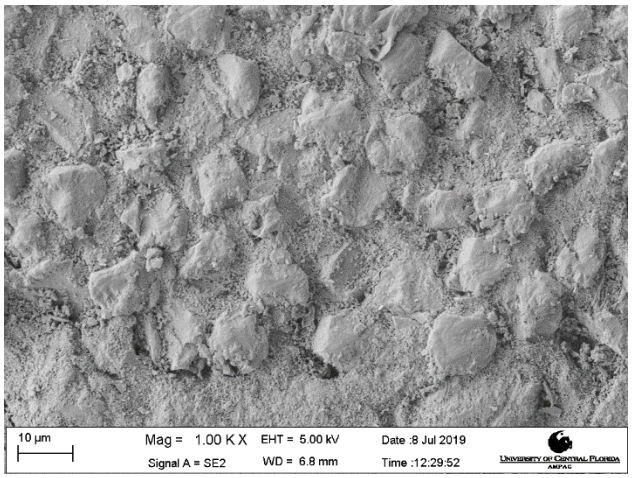

Fig 7b: Zoomed Secondary Electron view of same region as Fig 6a, revealed topography of surface

Comparing Fig. 3 and 6 the prepared sample showed no signs of delamination between layers. Each layer was comprised of two rows of fibers, one in the plane of the page and one coming out of the page. This was due to the plain weave pattern of the CMC utilized. Fig. 6 showed four of the six layers and no noticeable dark spots anywhere suggesting pore formation. Comparing Fig. 4 and 7 was extremely useful as it noted the damage morphology left by polishing on the cross sections of the fiber. Fig. 4 exemplified the actual geometry of the fibers within the matrix. Whereas, Fig. 7 indicated that the material removal must have impacted both the fiber and matrix features at the micro-scale as both are primarily composed of aluminum oxide. Polishing was a method of mechanical cutting and resulted in material removal at a small scale. It may be possible that smaller grits were utilized for too long causing the noted damage (fibers at cross section are not all circular). Utilizing finer grit for a longer time may have made the final material exposed much smoother due to finer cutting. This should be examined in future analysis as it is a limitation to the study and may be a cause for the lack of visible pore formation. Porosity is always present in a composite. It is possible SEM may not be able to measure the small amounts present in the sample, but other methods should be considered to evaluate the volumetric composition of CMC samples.

B. EDS

The EDS feature of this machine was limited to a lateral resolution of 5 microns which was significant as fibers were merely 10 to 12 micron in diameter. When line scans were performed the results varied between what should have been replicable results. Point scans performed showed consistent results across varied locations both matrix and fiber. These results were displayed in Fig. 8-10.

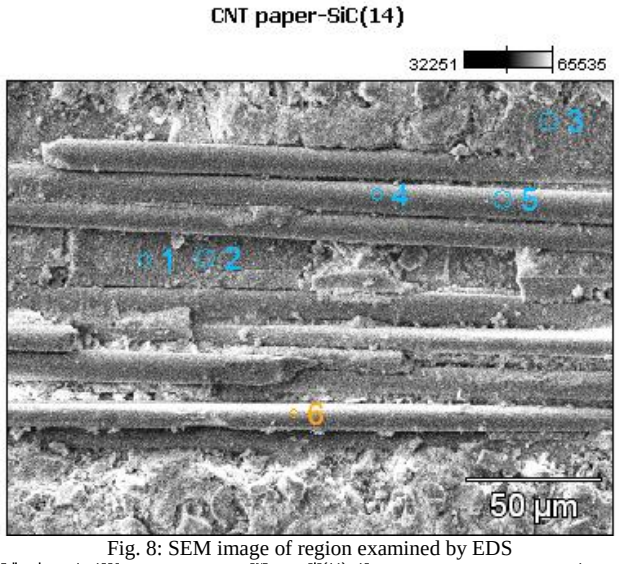

Fig. 8: SEM image of region examined by EDS

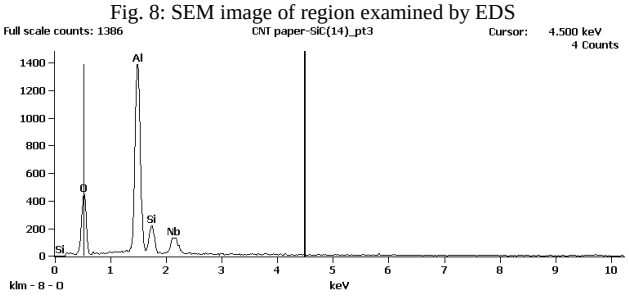

Figure 9: Peaks representative of matrix composition

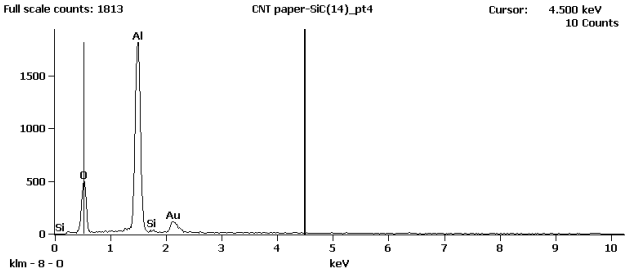

Figure 10: EDS peaks representative of fiber composition

The information from EDS confirmed the composition reported by manufacturer, both for matrix and fiber. The matrix had significantly more oxygen due to its aluminosilicate composition whereas fibers had notably higher counts of aluminum which confirms the aluminum oxide composition. This was significant as identified elements acted as the filter used in XRD analysis. Had any other dopant ions been present, it would have been incorporated to the analysis of XRD and its crystal structure.

C. XRD

The phase of the fiber was known to be alpha aluminum, however the matrix itself changed phase during pyrolysis. To ensure the reaction drove to completion XRD was performed on the matrix powder. Powder was extracted from fired samples. Samples were broken by hand and messaged to remove matrix material between layers. The resultant powder was sifted with a No.120 and No.200 mesh which filtered out particles over 75 micron in diameter. The powder was passed through the sieve a second time prior to analysis.

Fig. 11: Final matrix powder used for XRD analysis

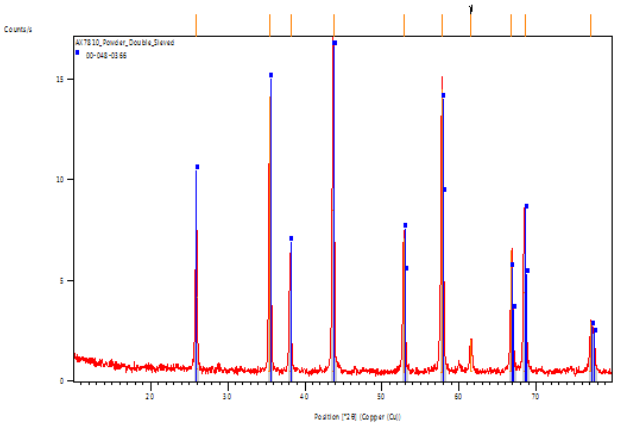

Fig. 12: XRD peaks of double sieved matrix powder
(X-axis: position 2θ Y-axis: Counts/s)

XRD results matched extremely close to the crystallographic planes defined by aluminum oxide peaks. The powder obtained resulted in peak intensities that were less commonly found in the data base. Most card files showed the greatest counts at the peak of 2θ of 35.5° with significantly less counts at 2θ of 43.7°. However, this is the opposite of what was repeatedly found with the matrix powder. Due to this consistency and peak not matched at 2θ of 61.6° some more data about the matrix phase should be examined. This may prove useful if the matrix phase is determined to be a less stable phase of aluminum oxide and could impact mechanical properties.

D. 3-pt bend

Samples were cut after autoclave treatment with a bandsaw by hand. Measurements were made with calipers and in accordance to ASTM C1341 [14]. The machining of the composite to reach the ASTM geometry was done by hand which resulted in some slight variation from sample to sample. Bending data was acquired using an electromechanical MTS Insight™ with 5kN maximum loading.

Fig. 13: Machine used to conduct 3-pt bending

The dimensions of the samples were incorporated to deduce the maximum flexural strength of the sample. Utilizing the bending equation, the maximum force applied was input to find the flexural strength of each sample.

$$\sigma = \frac{M * c}{I}$$

The given conditions of three-point bending were considered and simplified the equation.

$$\sigma = \frac{3}{2} * \frac{F_{max} * L}{bh^2}$$

TABLE 1: Calculated Flexural Strength

Trial	Maximum Force (N)	Flexural Strength (MPa)
1	21.358	85.432
2	23.979	95.916
3	25.688	102.752
4	20.898	83.592
5	27.907	111.628
STD	2.946	11.783
Average	23.966	95.864

In comparison to Axiom the sample tested had half as many layers and was composed of a fiber that was half as thin (thinner fibers or lower Denier coincides with improved flexion). The listed flexural strength for 1500D AX7810-610 was 275 MPa whereas the maximum strength calculated from the experiment was 111 MPa. This was alarming as it was only 40% of the reference value. When analyzing material properties there was nothing to suggest dramatically worse results in mechanical testing. Although ASTM standard corrected for differences in dimension: it is worthy to note the Axiom data sheet conducted testing with twelve layers of composite, whereas this test setup only utilized six layers. Flexural strength is a good indication of the performance of materials under structural loads. In order to verify the flexural strength calculated more testing will need conducted with further analysis of failure.

5. CONCLUSION

The research question was to determine the quality of CMC fabricated by the research lab. After analysis the material property confirmations suggested the fabricated samples were ready for mechanical testing. SEM displayed no signs of delamination or large pore formation at the cross-section face. EDS successfully confirmed fiber and matrix composition, aiding XRD analysis. XRD analysis resulted in peaks that matched closely with aluminum oxide, confirming the crystallinity of matrix phase formed. However, 3-point bend testing resulted in 40% of the claimed flexural strength claimed by Axiom.

Once the crystallinity, composition, and porosity were analyzed, the heat exchanger was developed. Fusion 360 was used to design the flange and mandrill parts to be machined from stainless steel (fig 123). These final parts would act as a mold over which the pre-preg would be wrapped over. Due to the nature of the 3-D layup a different bagging process will be utilized in which larger pleats will be used to allow the vacuum bag to conform to the curvature of the part.

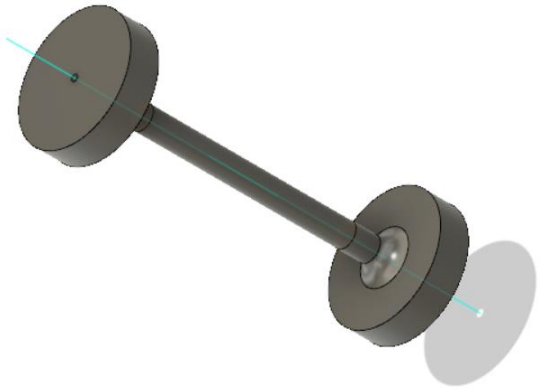
Fig. 14: CAD model of three-part modular mold for composite layup

SEM results of final cross section were more qualitatively useful rather than quantitatively descriptive. No pores were able to be identified via SEM. This is problematic as the composites volume is composed of matrix, fiber and some porosity. To claim 100% porosity would be inaccurate. This requires further testing and analysis to deduce the percent porosity present in the samples, as minimal as it may be. Sample preparation may be altered due to damage morphology of fibers, or alternate methods may be employed.

In the following weeks more bending tests will be conducted under ASTM C1341 specifications, with a depth a length ratio of 32:1. Due to previously poor test results, specimens of 12 layers will be fabricated for further testing. It may be possible that the CMC parts made are much more sensitive to thickness than is accounted for by ASTM standards. This will be analyzed by optical microscopy and SEM to confirm mode of failure after testing. Adjustments to testing will be made until results are comparable to that of the manufacturer (within 15%).

After room temperature bend test, tensile and interlaminar shear tests [15, 16, 17] will also need to be conducted at 24°C, 850°C, and 1000°C. These indicates the maximum operating temperature of most Inconel alloys prior to the onset of oxidation, as well as the maximum operating temperature of Nextel 610 fibers. Once evaluating thermo mechanical properties oxyacetylene torch testing can be conducted, as the test is relatively cheap, with easily reproducible results to compare with other thermally insulative materials [18]. Once all ASTM tests are completed the in-house manufacturing process will be well analyzed, allowing for accurate results regarding the final step.

The heat exchanger part will be the last piece to be tested. Tests will be done to analyze material degradation under operating temperatures of unique applications. The unique applications could range from aerospace hot sections, developing energy platforms, or even future heat exchange parts in nuclear reactors. Despite the application the fabricated part will be ideal for both chemically and thermally extreme environments.

ACKNOWLEDGEMENTS

I would like to thank the National Science Foundation (NSF) and Department of Defense (DoD) for this opportunity, as well as Robert Burke from the HYPER program. I appreciate Dr. Gordon and Jeremiah Juergensmeyer for opening their lab for mechanical testing. Thank you to Dr. Gou for his guidance, advise, and access to his composites' lab.

REFERENCES

[1] K.K. Chawla. "Composite Materials." New York: Springer Science + Business, 2012.

[2] Riccio. "Damage Growth in Aerospace Composites." New York: Springer Science + Business Media, 2015.

[3] National Research Council. "Chapter 1: Introduction" *Ceramic Fibers and Coatings: Advanced Materials for the Twenty-First Century*. Washington, DC: The National Academies Press. 1998.

[4] M.J. Walock, et al. "Ceramic Matrix Composite Materials for Engine Exhaust Systems on Next-Generation Vertical Lift Vehicles." *Journal of Engineering for Gas Turbines and Power*, vol. 140. 2018.

[5] J.D. Kiser, et al. "OXIDE/OXIDE CERAMIC MATRIX COMPOSITE (CMC) EXHAUST MIXER DEVELOPMENT IN THE NASA ENVIRONMENTALLY RESPONSIBLE AVIATION (ERA) PROJECT" *American Society of Mechanical Engineers*. Proceedings of the ASME Turbo Expo 2015: Ceramics GT2015 June 15-19, 2015, Montreal, Canada

[6] S.R. Levine. "Ceramics and Ceramic Matrix Composites- Aerospace Potential and Status." *American Institute of Aeronautics and Astronautics*. 33rd Structures, Structural Dynamics and Materials Conference, Dallas TX, United States, 1992

[7] K. Woo-Gon, et al. "Temperature effect on the creep behavior of alloy 617 in air and helium environments." *Nuclear Engineering and Design*, vol. 271, pp. 291-300, 2014.

[8] F. Feret, et al. "Determination of alpha and beta alumina in ceramic alumina by X-ray diffraction." *Spectrochimica Acta Part B: Atomic Spectroscopy*, vol. 55, pp. 1051-1061, 2000.

[9] Dr. G. Skandan, et al. "A New Class of Creep Resistant Oxide/Oxide Ceramic Matrix Composites." *NEI: Technical Report*, 2007.

[10] B. Jackson, A. Beaber, L. Visser, A. Barnes, J. Lincoln. "Oxide-Oxide Ceramic Matrix Composites - Enabling Widespread Industry Adoption." *9th International Conference on High Temperature Ceramic Matrix Composites*,, Vol. 263, 2016.

[11] S.Cox. "Processing and Characterization of Continuous Basalt Fiber Reinforced Ceramic Matrix Composites Using Polymer Derived Ceramics." M.S. thesis, University of Central Florida, United States, 2014.

[12] M.-L. Antti, E. Lara-Curzio, R. Warren. "Thermal degradation of an oxide fibre (Nextel 720)/aluminosilicate composite." *Journal of the European Ceramic Society*, vol. 24, pp. 565–578, 2004.

[13] V. Vasechko, F. Flucht, N. Rahner. "Mechanical investigation of weak regions in a wound oxide-oxide ceramic matrix composite." *Journal of the European Ceramic Society*, vol. 38, pp. 5192-5199, Dec. 2018.

[14] ASTM Standard C1341, 2013 (2018), "Standard Test Method for Flexural Properties of Continuous Fiber-Reinforced Advanced Ceramic Composites," ASTM International, West Conshohocken, PA, 2008, 10.1520/C1341-13R182, www.astm.org.

[15] ASTM Standard D3039, 2014 (2017), "Standard Test Method for Tensile Properties of Polymer Matrix Composite Materials," ASTM International, West Conshohocken, PA, 2017, DOI: 10.1520/D3039-D3039M-17, www.astm.org.

[16] ASTM Standard C1275, 2016 (2018), " Standard Test Method for Monotonic Tensile Behavior of Continuous Fiber-Reinforced Advanced Ceramics with Solid Rectangular Cross-SectionTest Specimens at Ambient Temperature," ASTM International, West Conshohocken, PA, 2018, DOI: 10.1520/C1275-18, www.astm.org.

[17] ASTM Standard D2344, 2013 (2016), " Standard Test Method for Short-Beam Strength of Polymer Matrix Composite Materials and Their Laminates" ASTM International, West Conshohocken, PA, 2016, DOI: 10.1520/D2344_D2344M-16, www.astm.org

[18] ASTM Standard E285, 2008 (2015), "Standard Test Method for Oxyacetylene Ablation Testing of Thermal Insulation Materials" ASTM International, West Conshohocken, PA, 2015, DOI: 10.1520/E0285-08R15, www.astm.org.